

Article

# Wildfire Effects on Groundwater Quality from Springs Connected to Small Public Supply Systems in a Peri-Urban Forest Area (Braga Region, NW Portugal)

Catarina Mansilha <sup>1,2,\*</sup>, Armindo Melo <sup>1,2</sup> , Zita E. Martins <sup>3</sup> , Isabel M. P. L. V. O. Ferreira <sup>3</sup>, Ana Maria Pereira <sup>1</sup> and Jorge Espinha Marques <sup>4</sup>

<sup>1</sup> National Institute of Health Dr. Ricardo Jorge, Department of Environmental Health, Rua Alexandre Herculano 321, 4000-055 Porto, Portugal; armindo.melo@insa.min-saude.pt (A.M.); ana.maria.pereira.95@gmail.com (A.M.P.)

<sup>2</sup> LAQV/REQUIMTE, University of Porto, Praça do Cel. Pacheco 42, 4050-083 Porto, Portugal

<sup>3</sup> LAQV/REQUIMTE, Department of Chemical Science, Food Science Laboratory and Hydrology, Faculty of Pharmacy, University of Porto, R. Jorge de Viterbo Ferreira 228, 4050-313 Porto, Portugal; zmartins@ff.up.pt (Z.E.M.); isabel.ferreira@ff.up.pt (I.M.P.L.V.O.F.)

<sup>4</sup> Institute of Earth Sciences and Department of Geosciences, Environment and Spatial Planning, Faculty of Sciences, University of Porto, Rua do Campo Alegre 1021, 4169-007 Porto, Portugal; jespinha@fc.up.pt

\* Correspondence: catarina.mansilha@insa.min-saude.pt; Tel.: +351-223401100

Received: 11 March 2020; Accepted: 15 April 2020; Published: 17 April 2020



**Abstract:** Peri-urban areas are territories that combine urban and rural features, being particularly vulnerable to wildfire due to the contact between human infrastructures and dense vegetation. Wildfires may cause considerable direct and indirect effects on the local water cycle, but the influence on groundwater quality is still poorly understood. The aim of this study was to characterize the chemistry of several springs connected to small public supply systems in a peri-urban area, following a large wildfire that took place in October 2017. Groundwater samples were collected in four springs that emerged within burned forests, while control samples were from one spring located in an unburned area. Sampling took place from October 2017 until September 2018, starting 15 days after the wildfire occurrence, to evaluate the influence of the time after fire and the effect of precipitation events on groundwater composition. Groundwater samples collected in burned areas presented increased content of sulfate, fluoride and nitrogen and variability in pH values. Iron, manganese and chromium contents also increased during the sampling period. Post-fire concentrations of polycyclic aromatic hydrocarbons (PAHs), mainly the carcinogenic ones, increased especially after intense winter and spring rain events, but the levels did not exceed the guideline values for drinking water.

**Keywords:** wildfire; peri-urban area; groundwater quality; polycyclic aromatic hydrocarbons; major ions; metals

## 1. Introduction

Wildfires are one of the main obstacles to the sustainability of forests and related ecosystems. The resulting devastation may cause severe economic and social costs, with the loss of lives and infrastructures, as well as the disturbance of the provision of goods and services, including ecosystem services, together with environmental damages such as the loss of carbon sequestration [1–3].

The urbanization of forest areas constitutes a new fire risk scenario. Over the years, throughout the world, the contact areas between human infrastructures and wild vegetation increased (the so-called peri-urban or wildland-urban interfaces) [4–6]. In Portugal, these areas result mainly from the

abandonment of croplands since the seventies, with fewer people to manage the land, creating great quantities of highly flammable combustible material, mostly from non-native species. This spatial pattern of human presence in the territory leads to particularly vulnerable areas to wildfire impacts, with disastrous consequences for populations and the environment [7,8]. Climate-related droughts and extreme weather are also propitious conditions for wildfires.

In 2017, Portugal suffered the greatest devastation caused by wildfires in a single year. Although in the last decades there have been a high number of fires, when compared to other countries and similar conditions, the wildfires that took place in 2017 largely exceeded the suppression capacity of the emergency services and were disastrous. Consequently, great damages occurred to population, with the loss of 115 lives, as well as to forests, rangelands, rural, industrial and urban areas. These catastrophic wildfires were worsened by climate change (it was the driest summer in nearly 90 years) and adverse meteorological conditions, and by the vegetation cover of fire-prone species, where the eucalyptus (*Eucalyptus globulus*) and maritime pine (*Pinus pinaster*) are dominant [2,9,10]. The burnt area was 539,921 ha, representing 498% of the average of the previous decennium, which was 90,269 ha, and nearly 60% of the total area burnt in the entire European Union, in which Portugal only represents about 2.1% of total landmass. The most critical month was October, with 3234 rural wildfires (15.4% of total annual rural wildfires) and 289,124 ha burnt (53.5% of total area). Wildfire occurrence prevailed mostly in the urban districts, often in peri-urban areas, which registered 55.6% of the total number of fires [10].

Regarding surface water and groundwater resources, the burning of forest catchments may result in a long-lasting legacy of water quality deterioration, whose magnitude and persistence can be observed from a few months to several years after the wildfire. Post-fire water quality concerns are complex and vary significantly from place to place depending on the severity, intensity, and duration of the fire, the soil and vegetation cover characteristics, the geological and geomorphological nature of the terrain, and the amount and intensity of precipitation during post-fire rain events [11,12]. Water quality impacts may also result from indirect effects associated with smoke and aerial deposition of ash [13,14].

According to the literature, wildfires may cause changes in several water quality parameters of interest or concern to water systems [11,15,16]. Contamination of streams and water reservoirs by post-fire inputs of suspended sediments and various trace elements present in ash may be problematic for both health and aesthetic reasons. High concentrations of iron (Fe), manganese (Mn), zinc (Zn), sodium ( $\text{Na}^+$ ) and chloride ( $\text{Cl}^-$ ) cause organoleptic problems (taste, color, staining of pipes and fittings). Sulfates ( $\text{SO}_4^{2-}$ ) have purgative effects for concentrations over 500 mg/L. Poisoning may occur from continued consumption of water containing high concentrations of copper (Cu), with gastrointestinal symptoms. Arsenic (As) and chromium (Cr) (specially hexavalent Cr) may be carcinogenic, while aluminium (Al), lead (Pb) and mercury (Hg) are toxic when consumed in sufficient quantities for prolonged periods. Following wildfire, increased exports of nitrogen (N) and phosphorous (P), in various forms, can also be problematic for managers of water supply catchments. High concentrations of nitrates ( $\text{NO}_3^-$ ) and nitrites ( $\text{NO}_2^-$ ) also present a potential risk to human health, primarily through reduction of  $\text{NO}_3^-$  to  $\text{NO}_2^-$ , which may affect oxygen transport in red blood cells, while high concentrations of ammonium  $\text{NH}_3^+/\text{NH}_4^+$  may corrode copper pipes and fittings. N and P are limiting nutrients for growth of aquatic plants, algae and cyanobacteria in water bodies. Eutrophication increases the risk of potentially toxic blooms, with implications for human health, aesthetic problems (taste, odor and color), and aquatic ecosystem function disturbance [14,17].

Polycyclic aromatic hydrocarbons (PAHs), such as benzo[a]pyrene, are known for their potential teratogenicity, carcinogenic and mutagenic properties, explained by the formation of adducts between the DNA bases and epoxides derived from hydrocarbons after an oxidizing process in the liver [18]. In addition to cancer, long-term exposition can also cause chronic bronchitis, skin problems and allergies. Some compounds are also classified as potential endocrine disruptors because they have estrogenic activity, generally coupled with a high potential for bioaccumulation [15,16,19,20]. The United States Environmental Protection Agency (USEPA) designated several PAHs as priority pollutants that should

be regulated due to their high toxicity and adverse effects [21]. PAHs were also designated as priority hazardous substances by the European Commission, in Directive on Environmental Quality Standards (Directive 2008/105/EC) [22].

The effects of fire on surface water are more evident than those on groundwater. Recharge rates, net infiltration and water balance can change after a wildfire, leading to difficulties in maintaining the supply of potable groundwater to populations [23]. Nowadays, despite the widespread access to tap water provided by the Portuguese municipalities, many people still prefer to drink groundwater from public fountains supplied by nearby springs, as it is associated with high purity and pleasant organoleptic characteristics. However, the impact of wildfires on the composition of groundwater from nearby springs is unknown.

The goal of this study was to identify the impact of the wildfire that occurred on October 2017, on the chemical characteristics of water from springs connected to small public supply systems used for human consumption in the peri-urban area of the city of Braga, in NW Portugal. The study included the analyses of major ions and trace elements, namely PAHs, which were carried out during one year after the wildfire.

## 2. Materials and Methods

### 2.1. Hydrogeological Framework

The city of Braga ( $41^{\circ}32' N$ ;  $8^{\circ}25' W$ ) is located in NW Portugal (Figure 1), in the Minho Province. The municipality has a resident population of 181,494 inhabitants (in 2011) [24], representing the seventh largest municipality in Portugal (by population) with an area of 183.40 km<sup>2</sup>. The city is surrounded by peri-urban areas consisting of agroforestry systems, especially in the higher and steeper terrain (Figures 1 and 2). To the southeast, the urban area is bordered by a mountainous ridge (Figure 1) with altitude above 500 m at the summits of Santa Marta (562 m), Monte Frio (548 m) and Sameiro (572 m). To the north, this region falls into the Cávado river catchment, while to the south it falls into the Ave river catchment.

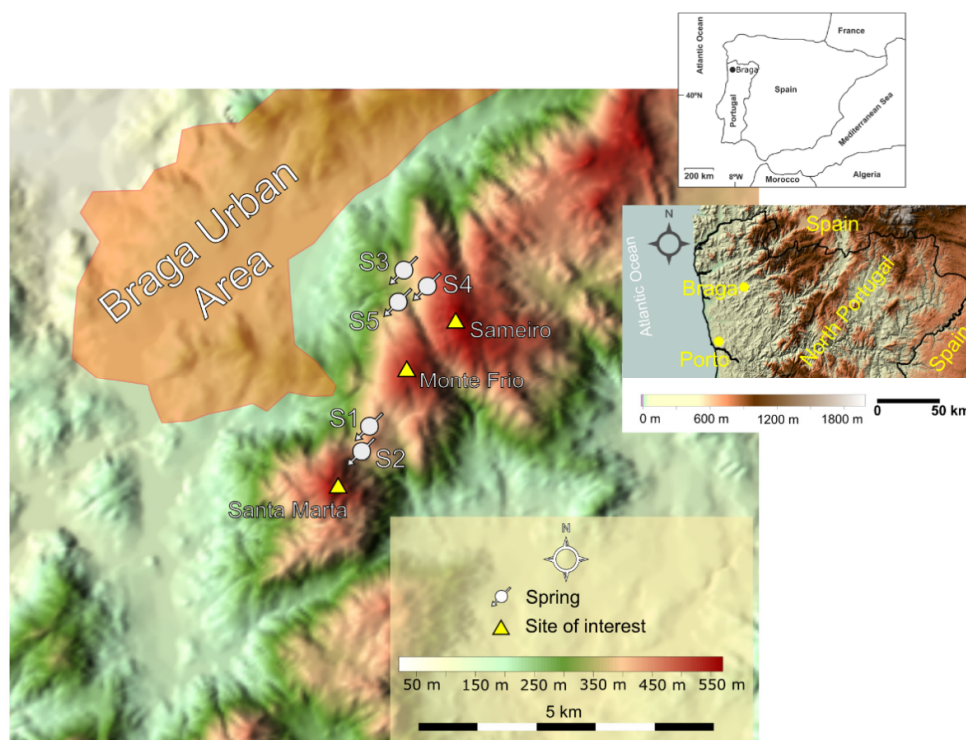


**Figure 1.** Location of Braga region in Iberia and in NW Portugal; hypsometric features of the study area; location of the studied springs.

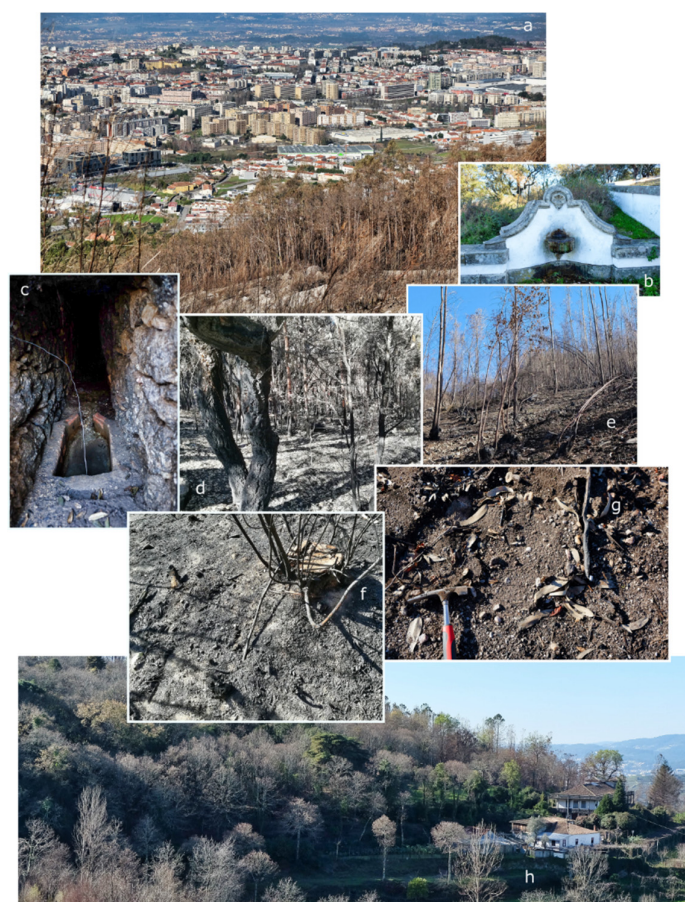


**Figure 2.** Some aspects of the study region: (a) burnt area of *Eucalyptus globulus* (first plan) and the Braga urban area (background); (b) Santa Maria Madalena sampling point (S1); (c) Monte de Dadim spring (S5); (d) *Quercus suber* burnt area at the vicinity of Santa Marta de Leão spring (S2); (e) *Eucalyptus globulus* burnt plantation at the recharge area of the Mina Spring; ash covered burnt soil immediately after the fire (f) and soil showing intense erosion one year after the fire (g); (h) deciduous forest at Monte de Dadim (S5, control point).

The Braga climate has Atlantic features, with a mean value of annual precipitation around 1449 mm at the local climatic station (located at 190 m of altitude). The temporal distribution pattern of precipitation is similar to the one usually observed in NW Portugal: December is the rainiest month (about 220 mm) and July is the driest month (about 22 mm). The mean annual air temperature is around 15 °C, with maximum in July and August (21 °C) and minimum in January (9 °C). The Braga Köppen–Geiger climate classification is Csb, which is dominant in Northwestern Iberia and corresponds to warm temperate (C), with dry and warm summer (sb) [25,26].

Braga region is located in the following geomorphological units [27]: Central System (1st level unit) and Entre Douro e Minho Open Valleys and Hills and Atlantic Front of NW Iberia Mountains (2nd level units). The region is also located in the Central-Iberian Zone of the Iberian Massif [28]. The dominant regional geological units are granitic rocks and metasedimentary rocks; sedimentary cover areas are residual. Therefore, the major processes in the local groundwater cycle take place mostly in fractured circulation media and, to a minor extent, in porous media.

The unsaturated zone depth often reaches more than 20 m at hilltops and less than 10 m at valley bottoms. In addition, the structure of the unsaturated zone encompasses a soil cover (mainly Leptosols, Regosols and Cambisols, with an umbric A horizon) overlying granite or metasedimentary rock.

## 2.2. Wildfire Description

Between 13 and 18 October of 2017, more than 7900 wildfires affected Northwestern Iberia. During this month, 15,440 wildfires were active, 33 of which were of important size, which spread quickly due to the drought and to particular meteorological conditions: strong winds caused by the Ophelia hurricane that swept the western coast of the Iberian Peninsula and unusual air temperatures, above 30 °C. September 2017 was the driest month in 87 years [29]. Around 81% of the territory was under severe drought and 7.4% in extreme drought. In the district of Braga, 23 wildfires were registered on 14 October and 43 wildfires on 15 October. The wildfire of greatest impact on the study region started in Leitões, Guimarães, and quickly reached Braga (particularly the mountain area between Santa Marta and Sameiro, see Figure 2), consuming over 1200 ha of forest [29].

The wildfire started at 13:00h on 15 October and was controlled within in a few hours. However, a strong reactivation projected the fire in several directions, with a very significant speed of propagation, and by 17:17h the authorities requested additional means to protect the houses, since the fire had two very long and intense fronts. Only by 10:09h, on 16 October, the wildfire was finally controlled [30].

## 2.3. Water Sampling

Groundwater samples were collected in springs that supply non-treated water used for human consumption, located in near Braga city (Figure 1): (i) Santa Maria Madalena Fountain (S1); (ii) Santa Marta de Leão Fountain (S2); (iii) Tanque de Dadim Fountain (S3); (iv) Depósitos Spring (S4); (v) Monte de Dadim Spring (S5). The recharge areas of S1 to S4 springs were affected by the wildfire, while S5 corresponds to a spring located in an unburned area, which was used as control.

All springs are characterized by relatively shallow water circulation. In fact, water is abstracted by means of hand dug galleries which, in this region, are typically associated with springs connected to the upper saturated zone and, sometimes, also to interflow. Moreover, springs S1 and S2 are located at hilltops and, therefore, have very short circulation paths. Finally, S3, S4, and S5 springs are all located at slopes and abstract water circulating in the granite weathering mantle.

The site selection criteria were the existence of permanent flow throughout the year, the location of the recharge areas regarding the burnt region, and the sampling feasibility. These sampling points were also chosen to be preserved as much as possible from other anthropogenic impacts, reducing the risk of water contamination by sources of pollution other than wildfires (Figures 1 and 2 and Table 1). The control spring analytical results were used to provide a framework of reference for contaminant concentrations on burned areas. The discharge flow in all springs was under 0.5 L/s.

**Table 1.** Features of the sampling points and the corresponding spring recharge areas.

Sampling Point	Altitude (m a.s.l.)	Lithology	Soil Types	Land Cover
S1—Sta. Maria Madalena Fountain	425	Metasedimentary rocks	Leptosol and Regosol	Public garden with <i>Quercus robur</i> and <i>Quercus suber</i>
S2—Sta. Marta de Leão Fountain	415	Granite	Leptosol and Regosol	Public garden and forest with <i>Quercus robur</i> , <i>Quercus suber</i> , <i>Pinus pinaster</i> and <i>Eucalyptus globulus</i>
S3—Tanque de Dadim Fountain	350	Granite	Regosol, Cambisol and Anthrosol	Deciduous forest
S4—Depósitos Spring	400	Granite (dominant) and metasedimentary rocks (residual)	Leptosol, Regosol and Cambisol	<i>Eucalyptus globulus</i> forest
S5—Monte de Dadim (control point)	390	Granite	Regosol and Cambisol	Deciduous forest

Samples collected at S1, S2, S3 and S4 were designated as Burnt samples (BR), and the ones collected at S5 as unburnt samples (NB). The sampling plan included five campaigns, carried out

during one year, from October 2017 until September 2018, starting 15 days after the wildfire occurrence (before the first post-fire rain event), and included 25 samples.

Samples were collected according to ISO 5667-3:2003(E) Water quality—Sampling—Part 3: guidance on the preservation and handling of water samples, during non-storm conditions, before and after the first overland flow event and aquifer recharge following the fire.

The influence of wildfire on water quality constituents was investigated. The physicochemical analyses of key water quality constituents included the major ions, organic matter and heavy metals, which may be mobilized according to fire intensity, post-fire precipitation, geological and geomorphological conditions and vegetation cover of each site. Compounds that can serve as specific markers, indicative of wildfire, such as the high molecular weight PAHs, were also monitored. Water pH, electrical conductivity (EC) and temperature were measured *in situ* during sampling.

The temporal distribution of precipitation and climate data (measured at Braga meteorological station) during the study period, provided the knowledge of the influence of rainfall on the input of pollutants into groundwater [31].

#### 2.4. Laboratory Analyses

Analyses were performed according to procedures outlined in *Standard Methods for the Examination of Water and Wastewater 23<sup>rd</sup> edition* and in *Le Rodier—L'analyse de l'eau 10<sup>e</sup> édition*. The laboratory has been accredited under ISO/IEC 17025 since 2007. Precision and accuracy were calculated for all analytical methods with values <10%. Uncertainties were also calculated with results varying from 2% to 10%.

Water turbidity was measured in a Hach 2100N Laboratory Turbidity Meter. Electrical conductivity (EC) and pH were determined in a Crison MultiMeter MM 41. Total alkalinity and total hardness were analyzed by titration and reported as milligrams per liter of calcium carbonate ( $\text{mgL}^{-1} \text{CaCO}_3$ ). Color,  $\text{PO}_4^{2-}$  and total phosphorus, expressed as P (TP) were analyzed in a Shimadzu UV-1601 Spectrophotometer (Shimadzu Corporation, Kyoto, Japan). Total nitrogen, expressed as N (TN) and chemical oxygen demand (COD), were evaluated in a Hach DR 2800 Spectrophotometer (Hach Company, Loveland, CO, USA). Major inorganic ions ( $\text{Na}^+$ ,  $\text{K}^+$ ,  $\text{Mg}^{2+}$ ,  $\text{Ca}^{2+}$ ,  $\text{Li}^+$ ,  $\text{Cl}^-$ ,  $\text{NO}_3^-$ ,  $\text{F}^-$  and  $\text{SO}_4^{2-}$ ) were analyzed by ion chromatography (Dionex<sup>TM</sup> system DX-120/ICS-1000, Dionex Corporation, Sunnyvale, CA, USA). Total organic carbon (TOC) was analyzed in a Shimadzu TOC-V (TOC-ASI-V, Shimadzu Corporation, Kyoto, Japan), heavy metals (Cr, Mn, Ni, Cu, Zn, As, Cd and Pb) and other components, such as Al, Fe,  $\text{NO}_2^-$ ,  $\text{NH}_4^+$  and  $\text{SiO}_2$ , were analyzed in a Varian AA240 Atomic Absorption Spectrometer (Varian Inc., Palo Alto, CA, USA) and in a Continuous Segmented Flow Instrument (San-Plus Skalar, Skalar Analytical, Breda, The Netherlands), respectively. PAHs were analyzed by dispersive liquid-liquid microextraction coupled to gas chromatography/mass spectrometry (DLLME-GC/MS) methodology in a Shimadzu GCMS-QP2010 gas chromatograph mass spectrometer equipped with an auto injector AOC5000 (Shimadzu Corporation, Kyoto, Japan), according the procedure described in Borges et al. [32].

Analytical standards were supplied by Sigma-Aldrich (Steinheim, Germany) and Merck (Darmstadt, Germany). The reference standard mixture containing the 15 EPA PAHs (acenaphthylene, Acy; acenaphthene, Ace; fluorene, Flu; phenanthrene, Phe; anthracene, Ant; fluoranthene, Flt; pyrene, Pyr; benz[a]anthracene, BaA; chrysene, Chr; benzo[b]fluoranthene, BbF; benzo[k]fluoranthene BkF; benzo[a]pyrene, BaP; dibenz[a,h]anthracene, DahA; benzo[ghi] perylene, BghiP; and indeno[1,2,3-cd]pyrene, Ind) was purchased from Sigma-Aldrich (Steinheim, Germany).

Methanol, dichloromethane and acetonitrile were organic trace analysis grade SupraSolv and were supplied by Merck (Darmstadt, Germany). Ultrapure water was highly purified by a Milli-Q gradient system ( $18.2 \text{ m}\Omega/\text{cm}$ ) from Millipore (Milford, MA, USA).

### 2.5. Statistical Studies

Data on chemical concentration was analyzed throughout time, location, and throughout time in burned areas. All dependent variables from every analyzed parameter were tested for distribution of the residuals with the Shapiro–Wilk’s test. Chemical concentrations were studied using a one-way analysis of variance (ANOVA), if normal distribution of the residuals was confirmed. Welch correction was applied when the homogeneity of variances was not verified. Whenever statistical significances were found, Tukey’s test or the Tamhane’s test post-hoc tests were applied for mean comparison, depending on variances assumption or not.

If normal distribution of the residuals was not found, parameters analyzed were studied using a Kruskal–Wallis test. Whenever statistical significances were found, Dunn’s post-hoc test was applied for median comparison.

All analyses were performed at 5% significance level, using XLSTAT for Windows version 2014.5 (Addinsoft, Paris, France).

## 3. Results and Discussion

The effects of wildfires on the catchment’s hydrologic responses were noted worldwide, although the specific impacts are unpredictable in terms of both the magnitude of potential effects and the persistence of the influence. So, there is no clear pattern for wildfire effects on water bodies, which may not be affected or, on the other hand, experience fire-related changes that can range from aesthetic concerns (taste or appearance) to potential toxicity or carcinogenicity with prolonged exposure, as well as environmental damages [14,33].

The concentration of major and trace elements monitored in groundwater collected at the peri-urban area of Braga, after the wildfire of October 2017, shown significant differences between samples for several compounds. However, for others, a clear tendency that could be attributed to the wildfire was not observed, or the variation over time was similar to that observed in control samples.

Post-fire analytical results are shown in Table 2 and corresponding statistical analysis on Supplementary Table S1.

The analyses of the results show a slight decrease followed by an increase in pH values in S1 and S2, and an increase in pH values in S3 and S4 during the sampling period, wherein 18 January and April 2018 were grouped, whereas the remaining sampling times were independent of each other ( $p = 0.006$ ). This is in accordance with studies that described wood ash as being alkaline and rich in carbonates and metal oxides [14]. However, ash chemical composition is highly variable as it reflects the type of vegetation and the part of the plant burned, as well as the soil type and combustion conditions, with different implications on water quality parameters [14,34]. No statistical differences ( $p > 0.050$ ) were found for turbidity, color and silica. The electrical conductivity, which is a water quality indicator for estimating the amount of mineralization and total dissolved solids, remained also constant during the study period, with no significant variations in BR samples ( $p > 0.050$ ).

Wildfires often induce quantitative and qualitative changes in soil organic matter, sometimes with significant losses due to the partial or total removal of the litter layer and, possibly, some organics from the upper few centimeters of mineral soil [35]. However, in this study, the total organic carbon concentrations appeared to be unaffected by fire, with mean values of  $0.37 \pm 0.15 \text{ mgL}^{-1}$  and  $0.33 \pm 0.17 \text{ mgL}^{-1}$  in BR and NB samples, respectively, and the chemical oxygen demand increased immediately after the fire, reaching a peak during spring, but then slowly declined as vegetation re-established. Nevertheless, these variations could not be attributed to the wildfire, as they occurred in the NB samples too ( $p > 0.050$ ).

**Table 2.** Physicochemical data of water samples from the studied region.

Sampling Point	Sampling Date	pH	COD	EC	Si	TP	HCO <sub>3</sub> <sup>-</sup>	F <sup>-</sup>	Cl <sup>-</sup>	SO <sub>4</sub> <sup>2-</sup>	PO <sub>4</sub> <sup>2-</sup>	NO <sub>3</sub> <sup>-</sup>	NO <sub>2</sub> <sup>-</sup>	NH <sub>4</sub> <sup>+</sup>	Na <sup>+</sup>	K <sup>+</sup>	Ca <sup>2+</sup>	Mg <sup>2+</sup>
		(mg/L)	(μS/cm)	(mg/L)	(mg/L)	(mg/L)	(mg/L)	(mg/L)	(mg/L)	(mg/L)	(mg/L)	(mg/L)	(mg/L)	(mg/L)	(mg/L)	(mg/L)	(mg/L)	(mg/L)
S1—Sta. Maria Madalena Fountain	17 October	6.0	2.5	37.1	8.5	0.05	10.1	0.02	6.6	0.4	0.067	<LD	0.007	0.006	5.7	0.6	1.7	0.5
	18 January	5.7	8.3	37.6	7.9	0.04	7.9	0.03	7.7	0.7	0.066	1.0	0.001	<LD	5.6	0.5	1.8	0.6
	18 April	5.5	10.1	41.7	6.9	0.04	5.0	0.09	9.0	1.5	<LD	2.0	0.005	0.002	6.8	0.4	0.5	0.4
	18 May	5.6	7.1	35.2	7.1	0.03	5.7	0.27	8.3	1.0	0.035	1.1	0.001	<LD	6.2	0.5	1.4	0.9
	18 September	6.3	5.6	34.9	9.3	0.12	8.8	<LD	6.9	1.3	0.041	0.8	0.002	<LD	5.2	0.8	2.0	0.5
S2—Sta. Marta de Leão Fountain	17 October	6.1	2.8	37.8	8.5	0.03	10.1	0.02	6.8	0.5	0.064	0.2	0.003	<LD	6.0	1.0	1.6	0.4
	18 January	5.8	8.6	37.2	7.8	0.06	7.3	0.04	7.7	0.7	0.070	1.1	<LD	<LD	5.6	0.5	1.8	0.6
	18 April	5.4	7.8	40.2	6.8	0.02	4.4	0.10	9.0	1.6	<LD	1.8	0.004	0.003	6.2	0.4	0.5	0.4
	18 May	5.6	5.4	34.2	7.1	0.24	5.7	0.28	8.5	1.1	0.014	1.6	<LD	<LD	5.8	0.5	1.3	0.7
	18 September	6.4	3.9	37.5	9.1	0.11	8.8	<LD	6.9	1.3	0.021	0.7	0.004	<LD	5.0	0.8	2.0	0.5
S3—Tanque de Dadim Fountain	17 October	5.6	2.9	48.4	15.4	0.05	15.7	0.02	7.7	<LD	0.260	0.5	0.003	<LD	7.9	0.8	2.0	0.6
	18 January	5.8	7.1	48.2	16.4	0.25	17.0	0.04	7.9	<LD	0.266	1.2	<LD	<LD	7.7	0.7	2.3	0.8
	18 April	6.1	9.1	47.0	16.3	0.07	12.6	0.05	7.7	0.5	0.118	0.8	0.004	0.011	8.5	0.7	1.8	0.5
	18 May	6.0	6.9	42.8	16.0	0.29	14.0	0.26	7.6	0.1	0.124	0.8	0.001	<LD	7.5	0.9	2.4	0.8
	18 September	6.3	5.9	46.7	17.0	0.19	15.3	<LD	7.4	0.8	0.146	0.7	0.002	<LD	6.7	0.8	2.3	0.7
S4—Depósitos Spring	17 October	5.6	2.1	61.6	10.6	0.05	26.5	0.02	8.5	<LD	0.121	4.7	<LD	<LD	7.5	0.6	4.0	1.1
	18 January	5.8	9.1	59.7	11.9	0.08	14.1	0.03	8.9	<LD	0.083	6.8	<LD	<LD	7.4	0.5	3.5	1.3
	18 April	5.9	8.5	61.8	12.1	0.04	12.6	0.05	9.3	0.8	0.282	7.5	0.006	0.005	9.0	0.6	2.9	1.2
	18 May	6.0	2.8	58.4	11.7	0.07	12.2	0.31	9.6	0.4	0.021	6.9	0.001	<LD	8.2	0.8	4.0	1.2
	18 September	6.7	2.9	58.7	11.9	0.06	13.5	<LD	8.8	1.0	0.060	5.5	0.004	0.001	6.5	0.8	3.2	1.2
S5—Monte de Dadim (control point, NB)	17 October	6.4	2.0	65.6	23.4	0.04	26.5	0.03	8.4	<LD	0.332	0.2	0.002	<LD	9.2	0.9	4.0	1.1
	18 January	6.7	7.1	65.0	23.4	0.36	28.4	0.06	8.3	<LD	0.337	0.8	0.001	<LD	8.7	1.0	4.5	1.2
	18 April	6.6	10.0	64.0	23.7	0.11	26.5	0.07	8.7	0.2	0.187	0.6	0.004	<LD	10.1	1.0	3.8	1.0
	18 May	6.4	5.8	59.8	22.6	0.11	23.6	0.11	8.4	<LD	0.200	0.6	<LD	<LD	7.5	0.6	3.0	1.5
	18 September	6.5	8.2	61.1	23.5	0.15	25.7	<LD	8.0	0.6	0.196	0.3	0.001	<LD	7.3	0.9	3.9	1.1

Analytical methods limits of detection (LD): 1.0 mg/L for COD; 0.8 μS/cm for EC; 1.78 mg/L for Si; 0.02 mg/L for TP and F; 0.3 mg/L for HCO<sub>3</sub>; 0.03 mg/L for Cl, SO<sub>4</sub>, NO<sub>3</sub>, Na, K, Ca, Mg; 0.01 mg/L for PO<sub>4</sub>; 0.001 mg/L for NO<sub>2</sub> and NH<sub>4</sub>.

Few compositional changes regarding major ions were observed. The Piper diagram presented in Figure 3 highlights the main changes: all sampling points reveal a minor shift from the first campaign (October 2017, at the end of the dry season) to the third campaign (April 2018, after the intense March precipitation events). The cations content shift results mainly from a decrease in calcium and an increase in sodium, while the anions content shift results from an increase in chloride and sulfate. However, changes in calcium and chloride ions observed in the burnt area are similar to those observed in the unburnt area and, thus, may not be connected to the wildfire. A decrease in bicarbonate is also observed in S1 to S4 points, but not in S5 point. Bicarbonate is originated by water–rock interaction and depends on the nature of the groundwater flowpaths that, in this case, are poorly known.

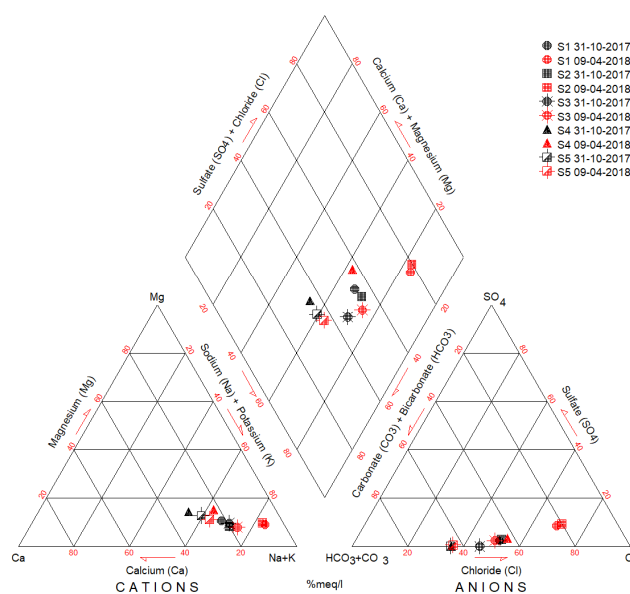


**Figure 3.** Piper diagram comparing the October 2017 campaign to the April 2018 campaign.

Regarding the sampling date, ANOVA analyses of major ions also reveal that chloride, sodium, potassium, calcium and magnesium concentrations did not vary significantly ( $p > 0.050$ ). In contrast, the increase of sulfate in groundwater from the burnt areas was statistically significant ( $p = 0.034$ ) and is probably due to the oxidation of sulfur in soil organic matter after the wildfire. Similar results were already observed in an earlier study carried out in Caramulo region, in Central Portugal [36] and reported in the literature by other authors [14].

The levels of fluoride have also risen ( $p = 0.003$ ) in May by approximately two orders of magnitude regarding the control point (S5), decreasing to levels similar to the initial ones in the last campaign.

Nutrient export from burnt soils usually increases after wildfires, and this process may affect groundwater composition. However, wildfire effects on stream exports of total phosphorus (TP) and total nitrogen (TN) vary significantly [14,37,38]. In the present study, it was observed a small decline (despite this, with no statistical significance) of phosphate, but an increase of TP with multiple change of 1.2 to 4.2 times the initial values. The wildfire effect on nitrogen should be examined with caution, because small differences regarding pre-fire values or control samples could be very important [39,40]. During the first six months after fire, the concentration of nitrogen species increased significantly ( $p < 0.001$ ), especially after precipitation, compared with concentrations in the reference samples. Combined concentrations of post-fire nitrite, nitrate and ammonium, which are dissolved forms, varied from  $0.52 \text{ mgL}^{-1}$  in control to  $6.28 \text{ mgL}^{-1}$  (mean values) in S4 sample. The land cover at the S4 recharge area consists only of forest, without other pollution sources besides the wildfire. The higher nitrate content observed in S4 should be a result of the wildfire and is in agreement with the thicker layer of ash observed in the recharge area of this spring. Several factors could explain the increase of

nitrogen exports in post-fire situations. On one hand, there is a lower plant demand and the nitrogen mineralization is stimulated (due to changes in pH and electrolytes). On the other hand, the nitrate form is mobile in soil-water systems and leaches through soil into catchments and drainages after heavy overland flow events that follow the wildfire [39,41]. In addition, because the wildfire removes forest cover and litter, rain interception decreases and nutrient transport via infiltration may increase. As well as nitrate, ammonium loading may increase as it is volatilized during fire and can dissolve into water. This compound may be retained in soil in its exchangeable form and subsequently be leached.

Hazardous chemicals, such as metals, were also monitored in Braga, as wildfires may influence the concentration of trace metals differently, with potentially harmful effects to human health and the environment. In this study no significant differences between samples collected in NB and BR locations were observed for cadmium (Cd), arsenic (As), lead (Pb), nickel (Ni), copper (Cu) and zinc (Zn). In contrast, the mean levels of iron (Fe), manganese (Mn) and chromium (Cr) were about 1.3, 7.0 and 2.8 times above the NB sample levels, respectively. Substantial post-fire increases in total iron and total manganese have been reported in the literature, indicating an added influx of these metals as part of an increase in particulates [42]. Even at values below the criteria established for aquatic systems, results must be considered as iron and manganese are related to aesthetic issues of the water (taste and color), and chromium, namely the hexavalent form, is carcinogenic. Concentrations of metals in groundwater samples are displayed in Table 3.

**Table 3.** Descriptive statistics of selected trace elements in groundwater samples after the wildfire.

		S1	S2	S3	S4	S5
Cd	Avg	0.07	0.02	0.02	0.06	<LD
	Min-Max	<LD–0.15	<LD–0.1	<LD–0.1	<LD–0.2	<LD
As	Avg	0.3	0.4	1.9	1.2	0.7
	Min-Max	<LD–0.8	<LD–0.6	1.6–2.4	0.7–2.3	0.2–1.3
Pb	Avg	0.04	<LD	0.5	<LD	<LD
	Min-Max	<LD–0.2	<LD	<LD–2.5	<LD	<LD
Ni	Avg	0.6	0.1	1.5	0.1	0.7
	Min-Max	<LD–3.0	<LD–0.4	<LD–6.7	<LD–0.4	<LD–3.0
Cu	Avg	3.1	0.8	2.0	2.3	2.4
	Min-Max	<LD–7.7	<LD–2.2	<LD–5.6	<LD–6.5	<LD–8.1
Zn	Avg	0.02	0.05	0.02	0.1	0.03
	Min-Max	<LD–0.1	<LD–0.2	<LD–0.1	<LD–0.1	<LD–0.2
Cr	Avg	0.8	0.26	0.2	0.2	0.1
	Min-Max	<LD–2.7	<LD–1.1	<LD–0.7	<LD–0.7	<LD–0.6
Fe	Avg	19.0	5.8	13.0	21.8	11.6
	Min-Max	6.1–55.5	<LD–13.5	<LD–13.8	<LD–56.0	<LD–25.5
Mn	Avg	2.6	2.9	0.5	2.4	0.3
	Min-Max	1.7–3.7	1.8–4.2	<LD–1.0	0.9–4.8	<LD–0.8

Min, Max, Avg, for minimum, maximum and average. Values of trace elements are in  $\mu\text{g/L}$ . Limits of detection (LD): 0.1  $\mu\text{g/L}$  for Cd, As, Pb, Ni, Cu, Zn and Cr; 5  $\mu\text{g/L}$  for Fe.

### PAH Analyses

This study also included the analyses of the 15 PAHs designated as priority hazardous pollutants. Thirteen hydrocarbons were found during the sampling period. The most abundant compounds in samples collected in burnt areas were Ant (26%), Acy (17%), BaA (15%) and BaP (14%), while in control samples Acy was the dominant compound (33%), followed by BaA (21%) and Ant (18%) (Figure 4). The sum of total concentrations, as well as the variety of PAHs, has increased throughout the year in all sampling points, with maximum values in May, after the wet season precipitation events. Mean values ranged from negligible amounts in S5 sample in January to  $0.029 \mu\text{g/L}^{-1}$  in S3 in May. Comparing the

initial to the last campaign, total values increased by factors of 1.3 to 2.2 times the initial concentrations. Furthermore, in control samples, only light PAHs, with three to four rings (Acy, Ace, Flu, Phe, Ant, Flt, Pyr, BaA, and Chr), were detected, in contrast to the samples of burnt areas, where a different profile was observed throughout the study period. Heavy PAHs, with five (BbF, BkF, BaP, and DahA) and six rings (InP, BghiP), have increased until May followed by a decrease in September, which probably indicates a natural remediation concerning these compounds. The compositional pattern of PAHs by ring size for the water samples is shown in Figure 5.

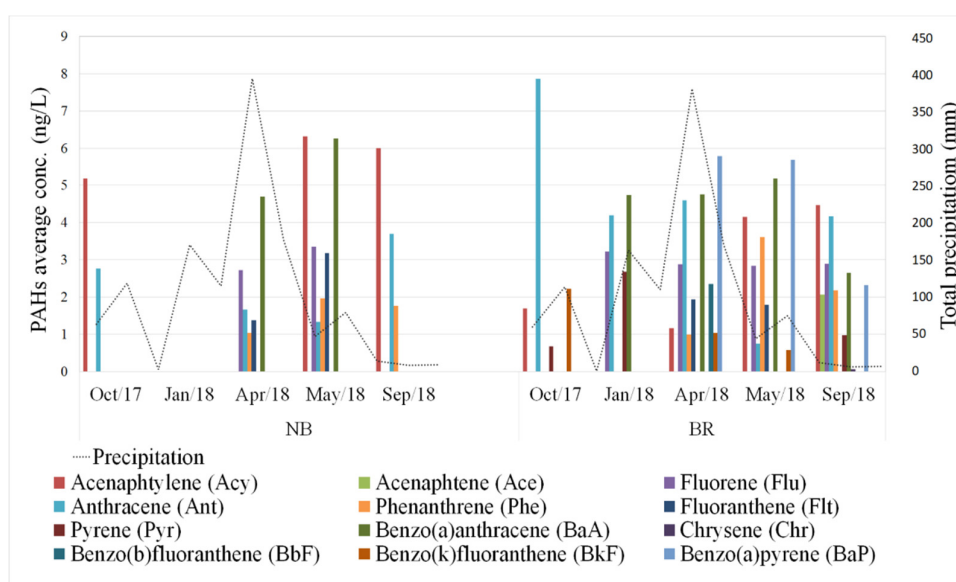


**Figure 4.** Average concentrations of polycyclic aromatic hydrocarbons (PAHs) (individual fractions) in S5 unburnt samples (NB) and in burnt areas (BR) (n = 4) and monthly precipitation.

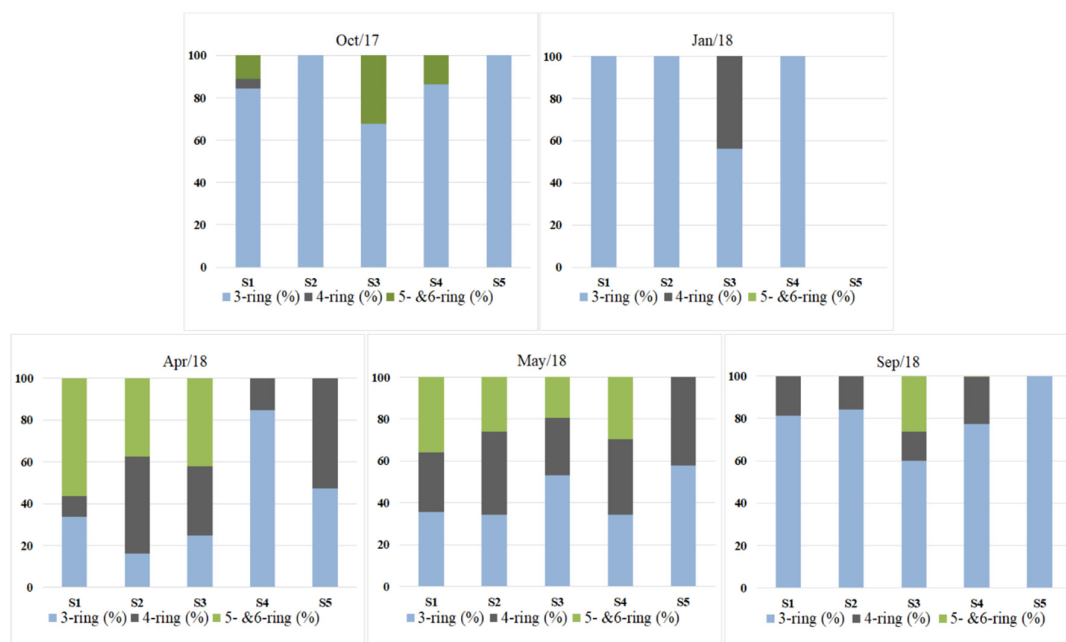


**Figure 5.** PAHs profiles of the samples collected in burned and control areas in the five sampling campaigns, according to their structural composition (number of benzene rings).

Significant differences for some PAHs were observed if the date of sampling was considered. Results from Shapiro–Wilk’s test shown that PAHs do not have a normal distribution of the residuals.

Kruskal–Wallis analysis for the sum of PAHs revealed that October 2017 and May 2018 sample results were significantly different. (Table S1).

Regarding the carcinogenic PAHs (BaA, Chr, BbF, BkF, BaP, Ind and DahA), the concentrations were also significantly higher in May 2018 ( $p = 0.022$ ), at levels around  $0.010 \mu\text{gL}^{-1}$  ( $0.0098$  to  $0.013 \mu\text{gL}^{-1}$ ) in BR samples, representing 60.4%, 52.9%, 36.2% and 62.6% of total PAHs in S1, S2, S3 and S4, respectively. Approximately half of these values correspond to BaP, with concentrations ranging from  $0.0046 \mu\text{gL}^{-1}$  in S4 to  $0.0077 \mu\text{gL}^{-1}$  in S1. In S3, concentrations of BaP increased in April 2018 and remained approximately constant up to September 2018, with a mean value of  $0.0052 \pm 0.0006 \mu\text{gL}^{-1}$ . In S5 samples (NB), BaP was not detected during the study period (Figure 6).

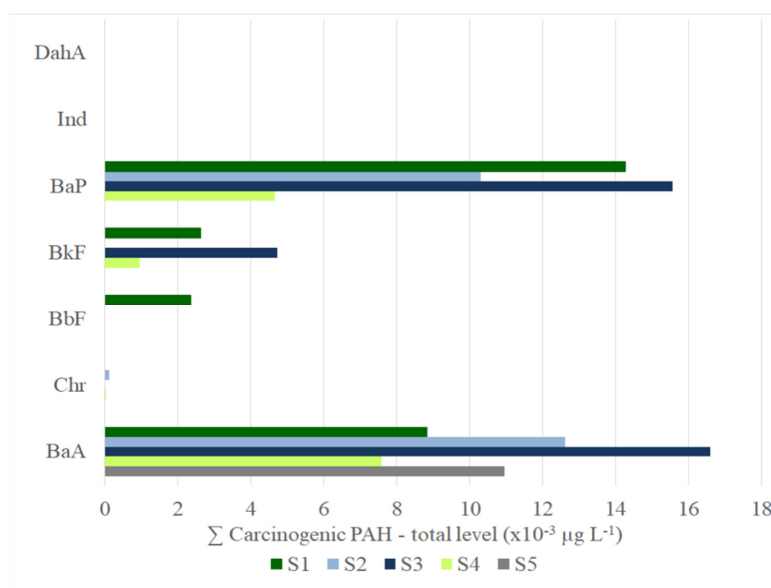


**Figure 6.** Total levels of carcinogenic PAHs (benz[*a*]anthracene (BaA), chrysene (Chr), benzo[*b*]fluoranthene (BbF), benzo[*k*]fluoranthene (BkF), benzo[*a*]pyrene (BaP), indeno[1,2,3-*cd*]pyrene (Ind) and dibenz[*a,h*]anthracene (DahA)) in NB (S5-control) and BR (S1 to S4) samples in the five campaigns.

Groundwater quality standards for PAHs (referred to as “threshold values”) were established by several European Member States taking into account identified risks [43]. Ranges of threshold values throughout Europe varied from  $0.005$  to  $0.03 \mu\text{gL}^{-1}$  for BaP,  $0.01$  to  $0.1$  for BghiP and BbF, and  $0.05$  to  $0.1 \mu\text{gL}^{-1}$  for BkF. Regarding these values, our results reveal several nonconformities for BaP, namely in samples collected in April and May in S1, S2 and S3. BaP, is the most extensively studied carcinogenic PAH, classified by IARC as a *Group 1* or a known human carcinogen [44], and is in the top ten priority pollutants designated by the Agency for Toxic Substances and Disease Registry (ATSDR) in 2015 [45]. BaP is also considered a powerful endocrine disruptor compound [46]. Despite the parametric value for drinking water established by the European Union Council Directive 98/83/EC for BaP has not been exceeded ( $0.010 \mu\text{gL}^{-1}$ ) [47], attention is needed especially regarding mixture cancer potency, as individual PAHs occur as part of environmental mixtures and cumulative risk assessment should be considered [48]. The established limit of  $0.100 \mu\text{gL}^{-1}$  for the sum of concentrations of BbF, BkF, BghiP and Ind was also not exceeded.

Regarding PAHs sources, they may have a pyrogenic origin, linked to processes of incomplete combustion of organic matter (in particular, vegetation or fossil fuels) or a petrogenic origin, resulting from the transformation of organic matter that occurs in geological materials [49]. Another source of PAH is the activity of plants, algae/phytoplankton, and microorganisms (biogenic PAHs) [50,51]. Diagnostic ratios based on PAHs physical and chemical properties and stability against photolysis can be used to distinguish between petrogenic and pyrogenic origins. Congener ratios of (Ant/Ant + Phe)

> 0.1 and  $(\text{Phe}/\text{Ant}) < 10$  indicate pyrogenic sources. The  $(\text{BaA}/\text{BaA} + \text{Chr})$  and  $(\text{Flt}/\text{Flt} + \text{Pyr})$  ratios are used to further distinguish combustion sources: high ratios ( $>0.35$  and  $>0.50$ , respectively) indicate grass, wood or coal combustion, intermediate ratios ( $0.20\text{--}0.35$  and  $0.40\text{--}0.50$ , respectively) indicate liquid fossil fuel combustion or mixed petrogenic and pyrogenic origin and low ratios ( $<0.20$  and  $<0.40$ ) usually imply petrogenic sources [52,53].

The ratios of  $(\text{Ant}/\text{Ant} + \text{Phe})$  and  $(\text{Phe}/\text{Ant})$  were calculated with results between  $0.68\text{--}0.82$  and between  $0.23\text{--}0.50$ , respectively, for samples in which PAHs were detected. The application of  $(\text{BaA}/\text{BaA} + \text{Chr})$  and  $(\text{Flt}/\text{Flt} + \text{Pyr})$  ratios was also performed, with values  $> 0.35$  and  $>0.50$ , also suggesting a pyrogenic source of PAHs (Figure 7).

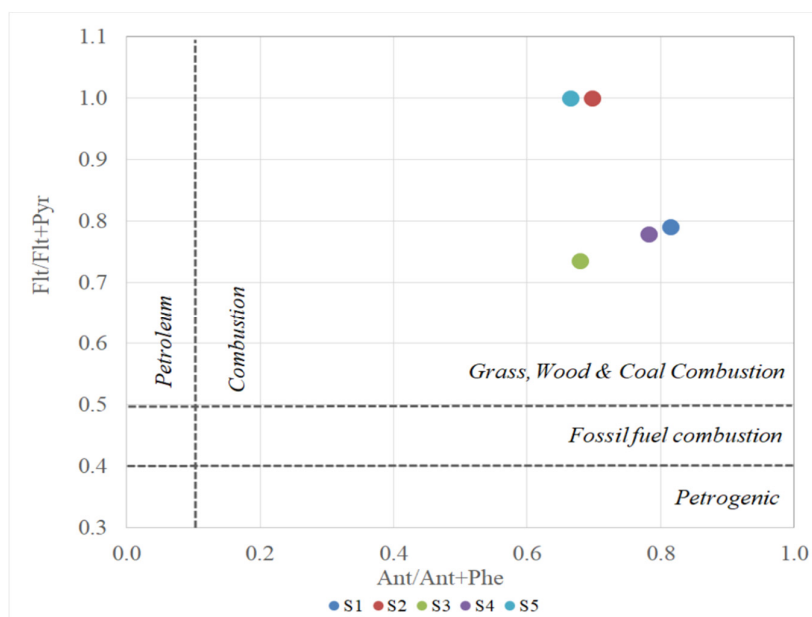


**Figure 7.** Ratios of (anthracene (Ant)/Ant + phenanthrene (Phe)) and (fluoranthene (Flt)/Flt + pyrene (Pyr)) for samples in which PAHs were detected.

#### 4. Conclusions

This study identified the main impacts of a large forest wildfire on groundwater quality of springs connected to small public supply systems in a peri-urban area. Results pointed out that the best practice for assessing wildfire hydrochemical effects is to start monitoring programs immediately after the wildfire event, and proceed with sampling campaigns for at least 12 months, since several parameters show considerable variation through time. It was also found that extreme events, like intense precipitation, were much more important for groundwater contamination than long-term average changes.

An increase in several parameters, such as sulfate, fluoride, phosphorous, nitrogen compounds, iron, manganese and chromium was observed in Braga peri-urban aquifers. Concerning PAHs, the results reflected the fire impact mainly through the profile of the compounds that appear in the BR springs, which differ significantly from the control spring. Six months after the wildfire, and after the first intense rain event, carcinogenic PAHs, including BaP, began to be detected in considerable concentrations, corroborating the idea of it being difficult to predict the long-term impacts of wildfires on groundwater quality.

Although the connection between groundwater depletion and destructive wildfires might seem tenuous at first glance, and the parametric values for drinking water established by international guidelines have not been exceeded, the results clearly demonstrate the vulnerability of aquifers to wildfires, especially for PAHs, which constitutes an issue yet poorly understood in terms of both the magnitude and persistence.

More information is needed on appropriate monitoring strategies in order to identify a standard set of trace and major compounds to be analyzed and establish protocols to effectively assess water quality, which is essential for developing sustainable water resources management practices.

**Supplementary Materials:** The following are available online at <http://www.mdpi.com/2073-4441/12/4/1146/s1>, Table S1: Values for statically analyses trends in the different sampling time for burned areas.

**Author Contributions:** Conceptualization, C.M. and J.E.M.; Data curation, C.M., A.M., Z.E.M., J.E.M.; Formal analysis, A.M., A.M.P.; Writing—original draft, C.M., A.M., J.E.M.; Writing—review and editing, C.M., I.M.P.L.V.O.F. All authors have read and agreed to the published version of the manuscript.

**Funding:** This work received financial support from the European Union (FEDER funds POCI/01/0145/FEDER/007265) and National Funds (FCT/MEC, Fundação para a Ciência e Tecnologia and Ministério da Educação e Ciência) under the Partnership Agreement PT2020 UID/QUI/50006/2013. The author J. Espinha Marques acknowledges the funding provided by the Institute of Earth Sciences (ICT), under contracts UIDB/04683/2020 with FCT (the Portuguese Science and Technology Foundation), and COMPETE POCI-01-0145-FEDER-007690.

**Conflicts of Interest:** The authors declare no conflict of interest.

## References

1. Chou, Y.H. Management of Wildfires with a Geographical Information-System. *Int. J. Geogr. Inf. Syst.* **1992**, *6*, 123–140. [[CrossRef](#)]
2. Turco, M.; Rosa-Cánovas, J.J.; Bedia, J.; Jerez, S.; Montávez, J.P.; Llasat, M.C.; Provenzale, A. Exacerbated fires in Mediterranean Europe due to anthropogenic warming projected with non-stationary climate-fire models. *Nat. Commun.* **2018**, *9*, 3821. [[CrossRef](#)] [[PubMed](#)]
3. Salis, M.; Ager, A.A.; Alcasena, F.J.; Arca, B.; Finney, M.A.; Pellizzaro, G.; Spano, D. Analyzing seasonal patterns of wildfire exposure factors in Sardinia, Italy. *Environ. Monit. Assess.* **2015**, *187*, 4175. [[CrossRef](#)] [[PubMed](#)]
4. Tartaglia, E.S.; Aronson, M.F.J.; Raphael, J. Does Suburban Horticulture Influence Plant Invasions in a Remnant Natural Area? *Nat. Area. J.* **2018**, *38*, 259–267. [[CrossRef](#)]
5. Bardsley, D.K.; Weber, D.; Robinson, G.M.; Moskwa, E.; Bardsley, A.M. Wildfire risk, biodiversity and peri-urban planning in the Mt Lofty Ranges, South Australia. *Appl. Geogr.* **2015**, *63*, 155–165. [[CrossRef](#)]
6. Esposito, G.; Parodi, A.; Lagasio, M.; Masi, R.; Nanni, G.; Russo, F.; Alfano, S.; Giannatiempo, G. Characterizing Consecutive Flooding Events after the 2017 Mt. Salto Wildfires (Southern Italy): Hazard and Emergency Management Implications. *Water* **2019**, *11*, 2663. [[CrossRef](#)]
7. Chas-Amil, M.L.; Touza, J.; Garcia-Martinez, E. Forest fires in the wildland-urban interface: A spatial analysis of forest fragmentation and human impacts. *Appl. Geogr.* **2013**, *43*, 127–137. [[CrossRef](#)]
8. Font, M.; Chauvin, S.; Plana, E.; Garcia, J.; Gladiné, J.; Serra, M. *Forest Fire Risk in the Wildland-urban Interface, Elements for the Analysis of the Vulnerability of Municipalities and Homes at Risk*; FIRECOM project (DG ECHO 2014/PREV/13); CTFC Editions: Solsona, Spain, 2016.
9. Vyklyuk, Y.; Radovanović, M.M.; Pasichnyk, V.; Kunanets, N.; Petro, S. Forecasting of Forest Fires in Portugal Using Parallel Calculations and Machine Learning. In *Recent Developments in Data Science and Intelligent Analysis of Information*; Springer: Cham, Switzerland, 2018; pp. 39–49.
10. JRC. *Forest Fires in Europe, Middle East and North Africa 2017*; Joint Research Centre (JRC): Ispra (VA), Italy, 2018.
11. Teclé, A.; Neary, D. Water Quality Impacts of Forest Fires. *J. Pollut. Eff. Cont.* **2015**, *3*, 1–7. [[CrossRef](#)]
12. Carignan, R.; D’Arcy, P.; Lamontagne, S. Comparative impacts of fire and forest harvesting on water quality in Boreal Shield lakes. *Can. J. Fish Aquat. Sci.* **2000**, *57*, 105–117. [[CrossRef](#)]
13. Miller, M.E.; Billmire, M.; Elliot, W.J.; Endsley, K.A.; Robichaud, P.R. Rapid Response Tools and Datasets for Post-Fire Modeling: Linking Earth Observations and Process-Based Hydrological Models to Support Post-Fire Remediation. *Int. Arch. Photogramm.* **2015**, *47*, 469–476. [[CrossRef](#)]
14. Smith, H.G.; Sheridan, G.J.; Lane, P.N.J.; Nyman, P.; Haydon, S. Wildfire effects on water quality in forest catchments: A review with implications for water supply. *J. Hydrol.* **2011**, *396*, 170–192. [[CrossRef](#)]
15. Yuan, H.; Tao, S.; Li, B.; Lang, C.; Cao, J.; Coveney, R.M. Emission and outflow of polycyclic aromatic hydrocarbons from wildfires in China. *Atmos. Environ.* **2008**, *42*, 6828–6835. [[CrossRef](#)]

16. Nunes, B.; Silva, V.; Campos, I.; Pereira, J.L.; Pereira, P.; Keizer, J.J.; Gonçalves, F.; Abrantes, N. Off-site impacts of wildfires on aquatic systems—Biomarker responses of the mosquitofish *Gambusia holbrooki*. *Sci. Total Environ.* **2017**, *581–582*, 305–313. [[CrossRef](#)] [[PubMed](#)]
17. WHO. *Guidelines for Drinking-Water Quality, Fourth Edition, Incorporating the 1st Addendum*; World Health Organization: Geneva, Switzerland, 2017.
18. Zuo, J.; Brewer, D.S.; Arlt, V.M.; Cooper, C.S.; Phillips, D.H. Benzo pyrene-induced DNA adducts and gene expression profiles in target and non-target organs for carcinogenesis in mice. *BMC Genom.* **2014**, *15*, 880. [[CrossRef](#)]
19. Albinet, A.; Leoz-Garziandia, E.; Budzinski, H.; Villenave, E. Polycyclic aromatic hydrocarbons (PAHs), nitrated PAHs and oxygenated PAHs in ambient air of the Marseilles area (South of France): Concentrations and sources. *Sci. Total. Environ.* **2007**, *384*, 280–292. [[CrossRef](#)]
20. Abdel-Shafy, H.I.; Mansour, M.S.M. A review on polycyclic aromatic hydrocarbons: Source, environmental impact, effect on human health and remediation. *Egypt. J. Petrol.* **2016**, *25*, 107–123. [[CrossRef](#)]
21. Keith, L.H. The Source of U.S. EPA's Sixteen PAH Priority Pollutants. *Polycycl. Aromat. Comp.* **2015**, *35*, 147–160. [[CrossRef](#)]
22. EC. *Directive 2008/105/EC of the European Parliament and of the Council on Environmental Quality Standards in the Field of Water Policy, Amending and Subsequently Repealing Council Directives 82/176/EEC, 83/513/EEC, 84/156/EEC, 84/491/EEC, 86/280/EEC and Amending Directive 2000/60/EC of the European Parliament and of the Council*; Official Journal of the European Union: Aberdeen, UK, 2008.
23. Moody, J.A.; Ebel, B.A.; Nyman, P.; Martin, D.A.; Stoof, C.R.; McKinley, R. Relations between soil hydraulic properties and burn severity. *Int. J. Wildland Fire* **2016**, *25*, 279–293. [[CrossRef](#)]
24. INE. *Censos 2011 Resultados Definitivos-Região Norte*; Instituto Nacional de Estatística, I.P.: Lisboa, Portugal, 2012.
25. AEMET-IM. *Atlas Climático Ibérico. Temperatura do Ar e Precipitação (1971–2000)*; Departamento de Producción da Agência Estatal de Meteorologia de Espanha (Área de Climatología y Aplicaciones Operativas) e Departamento de Meteorologia e Clima (Divisão de Observação Meteorológica e Clima), do Instituto de Meteorologia: Madrid, Spain, 2011.
26. Peel, M.C.; Finlayson, B.L.; McMahon, T.A. Updated world map of the Köppen-Geiger climate classification. *Hydrol. Earth Syst. Sci.* **2007**, *11*, 1633–1644. [[CrossRef](#)]
27. Pereira, D.M.I.; Pereira, J.S.P.; Santos, L.J.C.; França da Silva, J.M. Unidades geomorfológicas de Portugal Continental. *Rev. Bras. Geomorf.* **2014**, *15*, 567–584. [[CrossRef](#)]
28. Ribeiro, A.; Munhá, J.; Dias, R.; Mateus, A.; Pereira, E.; Ribeiro, L.; Fonseca, P.; Araújo, A.; Oliveira, T.; Romão, J.; et al. Geodynamic evolution of the SW Europe Variscides. *Tectonics* **2007**, *26*, TC6009. [[CrossRef](#)]
29. ICNF. *9.º Relatório Provisório de Incêndios Florestais -2017*; Departamento de Gestão de Áreas Públicas e de Proteção Floresta: Lisboa, Portugal, 2017.
30. Guerreiro, J.; Fonseca, C.; Salgueiro, A.; Fernandes, P.; Lopez Iglésias, E.; de Neufville, R.; Mateus, F.; Castellnou Ribau, M.; Sande Silva, J.; Moura, J.M.; et al. *Avaliação dos incêndios ocorridos entre 14 e 16 de outubro de 2017 em Portugal Continental. Relatório Final*; Comissão Técnica Independente, Assembleia da República.: Lisboa, Portugal, 2018.
31. IPMA. *Boletim Climatológico*; Instituto Português do Mar e da Atmosfera, I.P.: Lisboa, Portugal, 2018.
32. Borges, B.; Armino, M.; Ferreira, I.M.P.L.V.O.; Mansilha, C. Dispersive liquid–liquid microextraction for the simultaneous determination of parent and nitrated polycyclic aromatic hydrocarbons in water samples. *Acta Chromatog.* **2018**, *30*, 119–126. [[CrossRef](#)]
33. Martin, D.A. At the nexus of fire, water and society. *Philos. Trans. R. Soc. B* **2016**, *371*, 20150172. [[CrossRef](#)]
34. Andreu, V.; Rubio, J.L.; Cerni, R. Effect of Mediterranean shrub on water erosion control. *Environ. Monit. Assess.* **1995**, *37*, 5–15. [[CrossRef](#)] [[PubMed](#)]
35. Certini, G.; Nocentini, C.; Knicker, H.; Arfaioi, P.; Rumpel, C. Wildfire effects on soil organic matter quantity and quality in two fire-prone Mediterranean pine forests. *Geoderma* **2011**, *167*, 148–155. [[CrossRef](#)]
36. Mansilha, C.; Duarte, C.G.; Melo, A.; Ribeiro, J.; Flores, D.; Marques, J.E. Impact of wildfire on water quality in Caramulo Mountain ridge (Central Portugal). *Sustain. Water Resour. Manag.* **2017**, *5*, 319–331. [[CrossRef](#)]
37. Townsend, S.A.; Douglas, M.M. The effect of a wildfire on stream water quality and catchment water yield in a tropical savanna excluded from fire for 10 years (Kakadu National Park, North Australia). *Water Res.* **2004**, *38*, 3051–3058. [[CrossRef](#)]

38. Mast, M.A.; Clow, D.W. Effects of 2003 wildfires on stream chemistry in Glacier National Park, Montana. *Hydrol. Process.* **2008**, *22*, 5013–5023. [[CrossRef](#)]
39. Delwiche, J. After the Fire, Follow the Nitrogen. *JFSP Briefs.* **2010**, *80*. Available online: <http://digitalcommons.unl.edu/jfspbriefs/80> (accessed on 15 January 2020).
40. Ranalli, A.J. *A Summary of the Scientific Literature on the Effects of Fire on the Concentration of Nutrients in Surface Waters*; U.S. Geological Survey: Reston, VA, USA, 2004.
41. Rust, A.J.; Hogue, T.S.; Saxe, S.; McCray, J. Post-fire water-quality response in the western United States. *Inter. J. Wildland Fire* **2018**, *27*, 203–216. [[CrossRef](#)]
42. Sham, C.H.; Tuccillo, M.E.; Rooke, J. *Report on the Effects of Wildfire on Drinking Water Utilities and Effective Practices for Wildfire Risk Reduction and Mitigation*; Water Research Foundation and U.S. Environmental Protection Agency: Waltham, MA, USA, 2013.
43. EC. *Commission Staff Working Document Accompanying the Report from the Commission in Accordance with Article 3.7 of the Groundwater Directive 2006/118/EC on the Establishment of Groundwater Threshold Values*; European Commission: Brussels, Belgium, 2010.
44. IARC. *Agents Classified by the IARC Monographs, Volumes 1 to 113*; International Agency for Research on Cancer: Lyon, France, 2015; Volume 1–113.
45. ATSDR. *Priority List of Hazardous Substances*; Agency for Toxic Substances and Disease Registry: Atlanta, Georgia, 2015.
46. Hyzd'alova, M.; Pivnicka, J.; Zapletal, O.; Vazquez-Gomez, G.; Matthews, J.; Neca, J.; Pencikova, K.; Machala, M.; Vondracek, J. Aryl Hydrocarbon Receptor-Dependent Metabolism Plays a Significant Role in Estrogen-Like Effects of Polycyclic Aromatic Hydrocarbons on Cell Proliferation. *Toxicol. Sci.* **2018**, *165*, 447–461. [[CrossRef](#)]
47. EC. *Directive 98/83/EC on the Quality of Water Intended for Human Consumption*; Official Journal of the European Union: Aberdeen, UK, 1998.
48. MDH. *Guidance for Evaluating the Cancer Potency of Polycyclic Aromatic Hydrocarbon (PAH) Mixtures in Environmental Samples*; Minnesota Department of Health: St. Paul, MN, USA, 2016.
49. Stogiannidis, E.; Laane, R. Source Characterization of Polycyclic Aromatic Hydrocarbons by Using Their Molecular Indices: An Overview of Possibilities. *Rev. Environ. Contam. Toxicol.* **2015**, *234*, 49–133.
50. Denis, E.H.; Toney, J.L.; Tarozo, R.; Scott Anderson, R.; Roach, L.D.; Huang, Y. Polycyclic aromatic hydrocarbons (PAHs) in lake sediments record historic fire events: Validation using HPLC-fluorescence detection. *Org. Geochem.* **2012**, *45*, 7–17. [[CrossRef](#)]
51. Nasher, E.; Heng, L.Y.; Zakaria, Z.; Surif, S. Concentrations and Sources of Polycyclic Aromatic Hydrocarbons in the Seawater around Langkawi Island, Malaysia. *J. Chem.* **2013**, *2013*, 975781. [[CrossRef](#)]
52. Edokpayi, J.; Odiyo, J.; Popoola, O.; Msagati, T. Determination and Distribution of Polycyclic Aromatic Hydrocarbons in Rivers, Sediments and Wastewater Effluents in Vhembe District, South Africa. *Int. J. Environ. Res. Public Health* **2016**, *13*, 387. [[CrossRef](#)] [[PubMed](#)]
53. Yunker, M.B.; Macdonald, R.W.; Vingarzan, R.; Mitchell, R.H.; Goyette, D.; Sylvestre, S. PAHs in the Fraser River basin: A critical appraisal of PAH ratios as indicators of PAH source and composition. *Org. Geochem.* **2002**, *33*, 489–515. [[CrossRef](#)]

